Balance strategy in hoverboard control

Mohammad Shushtari (smshushtari@uwaterloo.ca)
University of Waterloo
Atsushi Takagi
NTT (Japan)
Judy Lee
Imperial College London
Etienne Burdet
Imperial College London
Arash Arami
University of Waterloo

Research Article

Keywords: center of pressure (COP), center of gravity (COG), COM, static balance, LPSI/RPSI, LKNE/RKNE, Tibialis Anterior (TA), Gastrocnemius Medial Head (GMH), Biceps Femoris (BF)

Posted Date: June 17th, 2021

DOI: https://doi.org/10.21203/rs.3.rs-618490/v1

Version of Record: A version of this preprint was published at Scientific Reports on March 16th, 2022. See the published version at https://doi.org/10.1038/s41598-022-08291-0.

Balance strategy in hoverboard control

Mohammad Shushtari[1,*], Atsushi Takagi[2], Judy Lee[3], Etienne Burdet[3], and Arash Arami[1,4,*]

[1]Department of Mechanical and Mechatronics Engineering, University of Waterloo, Waterloo ON, Canada
[2]NTT Communication Science Laboratories, 3-1 Morinosato Wakamiya, Atsugi, Kanagawa, 243-0198, Japan
[3]Department of Biomedical Engineering, Imperial College of Science, Technology and Medicine, London, UK
[4]Toronto Rehabilitation Institute, University Health Network, Toronto, ON, Canada
[*]Corresponding authors: smshushtari@uwaterloo.ca, aarami@uwaterloo.ca

ABSTRACT

This work investigates how people learn to perform lower limb control in a novel task with a hoverboard which requires maintaining dynamic balance. An experiment was designed to investigate the learning of balance and control strategies: i.e. hip versus ankle strategy. Motor learning was indicated by a decrease in total muscle activation and time to complete a trial. The results further show that participants with no prior experience of riding a hoverboard learn an ankle strategy to maintain their balance and control the hoverboard. This is supported by significantly stronger phase synchrony and lower dynamic time warping distance between the hoverboard plate orientation, that controls hoverboard motion, and the ankle angle when compared to the hip angle. A decrease of 14.2% in the co-activation of the muscles acting on the ankle joint also confirms the adoption of the ankle strategy. The adopted ankle strategy is robust to the foot orientation despite salient changes in muscle group activation patterns.

Introduction

Balance control integrates sensory information from the visual, vestibular, and somatosensory systems[1–3] and involves different spinal and supraspinal reflex circuits, reticulospinal descending tract, and cortical control of upper and lower limbs. From a biomechanical perspective, balance control is divided into static and dynamic categories. In static balance, equilibrium is maintained by modulating the center of pressure (COP) such that the body's center of gravity (COG) is always kept within the base of support. In dynamic balance, the COG goes out of the base of support, however, the equilibrium is re-established consecutively[4].

Dynamic balance is essential for daily locomotion and sports activities. It plays an important role in snowboarding[5] and the control of new means of transportation such as hoverboard and Segway[6–8]. In contrast to the Segway, the hoverboard provides no stability by itself and the stability yields by the user in-the-loop, making the balance control more challenging. Hoverboard balance resembles the balance control in quiet standing in the anterior/posterior direction where feet are placed stationary side by side. In quite standing, human uses mainly ankle and hip based balance strategies for maintaining equilibrium. In ankle strategy, equilibrium is achieved by tilting the body about the ankle joint. Hence, the ankle's agonist and antagonist muscles are primarily activated to regulate the COG by performing plantarflexion/dorsiflexion rotations. In contrast, in the hip strategy, balance is maintained as a result of the hip flexion/extension, which results in movement of COM in anterior/posterior directions. Therefore, in the hip strategy, the ankle joint produces smaller torques comparatively and its muscles are almost unresponsive[4,9]. As balance requires postural control about unstable equilibrium (we simply fall if we are perturbed from upright posture and axial muscles are not activated), it requires learning to yield the appropriate strategy to control the mechanical impedance at different joints[10], which can be achieved through selective muscle co-activation. Recent studies targeted identifying the mechanical impedance at hip and ankle in a static posture[11–13] and during walking[14,15].

Maintaining balance on a hoverboard is similar to stabilizing a cart-pendulum system while the human balance in quiet standing is comparable with stabilizing an inverted pendulum[16]. Compared to quiet standing where the COG is kept within the base of support using ankle and hip strategies (static balance), COG in hoverboard riding is pushed outside of the base of

support (dynamic balance) to accelerate the hoverboard. Hoverboard acceleration is then modulated by the rider to maintain equilibrium and control the position or velocity of the hoverboard simultaneously. Despite this fundamental difference between quiet standing and hoverboard balance, they are similar in the sense that human feet are stationary placed on the ground or hoverboard plates. Therefore, similar strategies are expected to emerge for maintaining the dynamic balance in hoverboard control as in quiet standing.

Hoverboard control is also a redundant task that involves ankle, knee, and hip joints simultaneously. It enables us to study how people resolve this redundancy while controlling a hoverboard and which balance strategy they utilize. The potential of riding a hoverboard in balance assessment and improvement is also not yet investigated. In this full-body dynamic task, we examine which balance strategy is adopted riding a hoverboard, how motor learning emerges in first-time users and what metrics indicate better riding performance. Finally, we investigate the robustness of this strategy to changes of lower limb posture and task kinematics and analyze muscle activation patterns in different conditions.

Methods

Experimental setup

A hoverboard (Bluefin Classic Scooter, UK) was used for the experiment, which comes equipped with two 350W brush-less DC motors and reaches a maximum speed of 16 km/h. A hoverboard can be modeled as a cart pendulum system where its movements are generated in the direction of the applied tilt to its plates (Figure 1A). In particular, the hoverboard speed is controlled by the tilt angle. 10 MX13+ Cameras (Vicon, UK) were used to capture the kinematics of the hoverboard and participants' lower limbs at 150Hz. Furthermore, a setting of "PlugInGait" with 16 markers was used to calibrate and label the participant's lower limb. Markers were placed on the left/right anterior superior iliac spine (LASI/RASI), left/right posterior superior iliac spine (LPSI/RPSI), the lower lateral 1/3 surface of the left/right thigh (LTHI/RTHI), the flexion-extension axis of the left/right knee (LKNE/RKNE), the lower 1/3 surface of the left/right shank (LTIB/RTIB), the lateral malleolus along an imaginary line that passes through the transmalleolar axis of left/right ankle (LANK/RANK), the calcaneus at the same height above the plantar surface of the left/right foot as the toe marker (LHEE/RHEE), and the second metatarsal head, on the mid-foot side of the equinus break between fore-foot and mid-foot of the left/right leg (LTOE/RTOE). Two additional markers were placed on the hoverboard extremities in order to measure its movement using motion capturing.

Eight wireless electromyography (EMG) sensors (Trigno, Delsys, USA) with a sampling rate of 3000Hz were placed on the following muscles of both legs: Tibialis Anterior (TA), Gastrocnemius Medial Head (GMH), Biceps Femoris (BF), Rectus Femoris (RF). EMG sensors were placed on the skin after shaving and skin surface cleaning with ethanol. Motion capture system and EMG sensors were also calibrated and synchronized.

Experimental protocol

All participants signed informed consent forms before participating in the study. Study protocols and procedures were all approved by the University of Waterloo (ORE#40451), Clinical Research Ethics Committee and conformed with the Declaration of Helsinki. 10 participants (age: 21.9 ± 0.74 years, and 5 females) without known sensorimotor impairment and without previous experience in riding a hoverboard or similar self-balanced equipment were recruited. They went through a 5-minute familiarization with the hoverboard to learn how to step up and down from it, stabilize their balance, and move and turn with no specific instruction.

Two parallel lines (Bottom line and Top line) were color taped on the ground with a distance of 0.6m to be visible to the hoverboard riders. Starting from the middle of the Bottom line, all participants were asked to perform accurate goal-directed movements between two lines (Figure 1E). Forward movement is defined from the Bottom line to the Top line and backward movement from the Top to the Bottom line. A forward followed by a backward movement is considered a trial.

In the first condition experimented (A1), participants were asked to stand on the hoverboard with their feet tilted at 45° to their left (Figure 1B). In the second condition (B), executed after A1 trials, they were asked to perform the same movement with their feet oriented at 45° to their right (Figure 1D). The third condition (A2) was repetition of the first condition. The maximum voluntary contraction (MVC) of each muscle was recorded to normalize the EMG signals[17] and foot posture was checked before start of each condition. In each of the conditions, participants were asked to perform the maximum number of

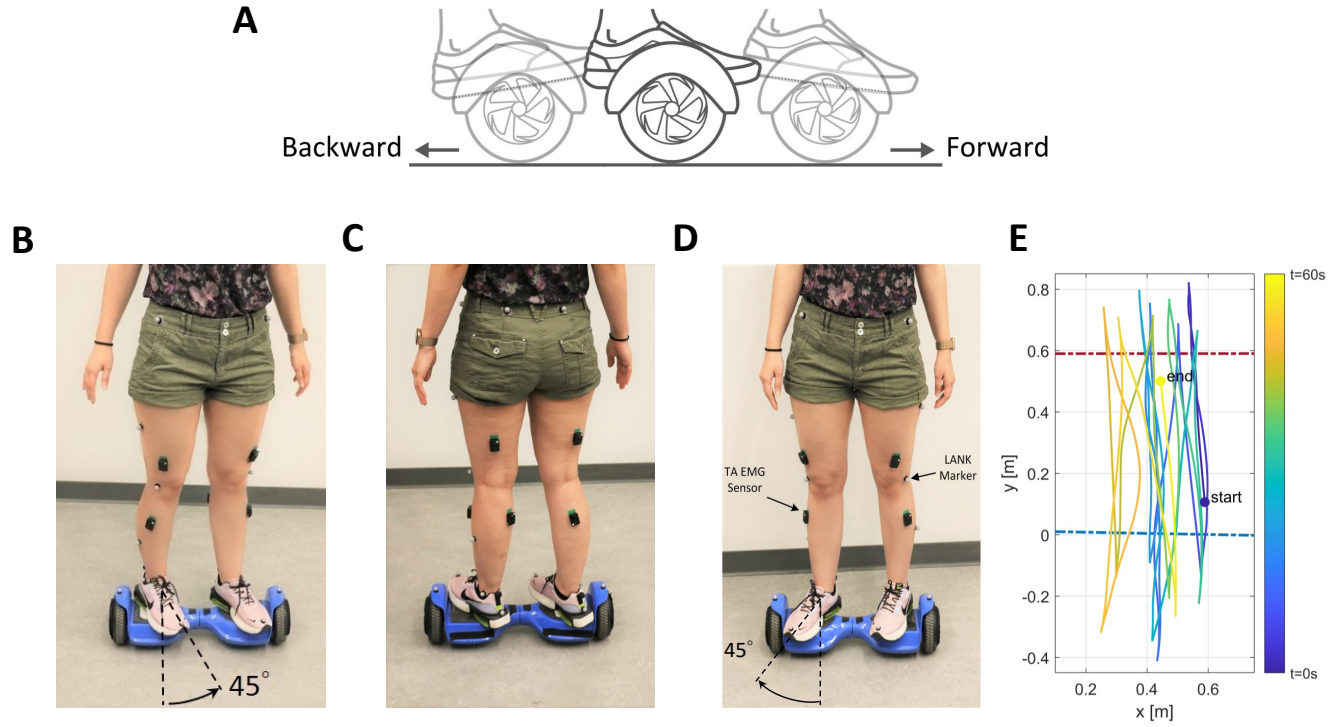

Figure 1. (**A**) Hoverboard forward and backward motion according to the applied tilt. (**B** and **C**) Participant wearing sixteen reflective markers and eight wireless EMG sensors while standing on hoverboard with foot oriented 45° to the left in condition A1 and A2 from anterior and posterior view, respectively. (**D**) participant with foot oriented 45° to the right in condition B. (**E**) Sample movement trajectory of a representative participant #9 in condition A2 in x-y plane. The line color represents the trial time. The Top and the Bottom lines are depicted with red and blue dashed lines, respectively.

trials they could in 60 seconds. One of the participants failed to perform the trials, and so was excluded from the analysis.

Data analysis

Preprocessing

The data from the motion capture system and EMG sensors were split into half-trials (forward/backward motion in each trial). This segmentation was carried out based on the hoverboard position computed on the data from the markers fixed on the hoverboard smoothed using a moving average filter with a 0.67-second window.

EMG signals were filtered with a third-order Butterworth bandpass filter with cutoff frequencies of 30Hz and 450Hz, respectively. After rectification, their RMS values were computed using a moving RMS filter with a one-second window. Next, each signal was normalized to its corresponding MVC value, and finally, each muscle onset/offset was computed using thresholds defined by multiple standard deviations of EMG-baseline noise[17].

Hoverboard control performance analysis

We considered the trial elapsed time as a performance measure since participants were asked to perform as many trials as they could in a minute. We used a Linear Mixed Model (LMM) to analyze the performance and motor learning patterns of participants. We included the condition (A1, B, and A2) and movement direction (forward and backward) as fixed effect intercepts, and treated the trial number as a fixed slope. To account for the correlation of repeated measurements within each participant, a random intercept and slope with respect to the trial number are also considered. Thus, the trial elapsed time (T_{im})

for a given observation i on participant m was modeled as

$$T_{im} = \beta_0 + \beta_1 \mathrm{B}_i + \beta_2 \mathrm{A2}_i + \beta_3 \mathrm{backward}_i + \beta_4 \mathrm{trial}_i + b_{0m}\mathrm{sub}_{im} + b_{1m}(\mathrm{trial}_{im}, \mathrm{sub}_{im}) + \varepsilon_{im}. \quad (1)$$

The indicator variables B_i, $\mathrm{A2}_i$, and $\mathrm{backward}_i$ were set to one, if observation i belonged to the respective condition or direction, otherwise to zero. The slope variable trial_i was also equal to the trial number. Similarly, trial_{im} and sub_{im} were set to the trial number and one, respectively, in case the observation i belonged to the participant m, otherwise were set to zero. ε_{im} captures the difference between the measured values (T_{im}) and the prediction of the model for participant m.

EMG signal processing

The muscle co-activation between muscles p and q in the trial i (C^i_{pq}), was computed as:

$$C^i_{pq} = \frac{\int_{t^i_{\mathrm{start}}}^{t^i_{\mathrm{end}}} e_p(t)\, e_q(t)\, dt}{t^i_{\mathrm{end}} - t^i_{\mathrm{start}}}$$

where e_p and e_q are the filtered, normalized EMG signals of muscles p and q, respectively. Setting $p = q$, we can compute the mean square muscle activation for each muscle. Among six different combinations of muscles for co-activation calculation, only three of them are interpreted: C_{12} between Bicep Femoris and Gastrocnemius Medial Head, C_{13} between Bicep Femoris and Rectus Femoris, and C_{24} between Tibialis Anterior and Gastrocnemius Medial Head. C_{12} and C_{13} are related to the muscles that exert agonist-antagonist torques on the knee joint, which we call knee co-activation type 1 and 2, respectively. Similarly, we call C_{24} the ankle co-activation since it is related to the muscles that exert agonist-antagonist torques on the ankle joint. C_{11}, C_{22}, C_{33}, and C_{44} are also the muscle activation of Bicep Femoris, Gastrocnemius Medial Head, Rectus Femoris, and Tibialis anterior, respectively. The total muscle activation was also computed as $C_{\mathrm{Total}} = \sum_{j=1}^{4} C_{jj}$. Furthermore, to evaluate the effort during a trial, we used the measure

$$W = \int_{t_{\mathrm{start}}}^{t_{\mathrm{end}}} \left(\sum_{p=1}^{4} e_p(t) \right) . |v_{\mathrm{hb}}|\, dt$$

where v_{hb} is the hoverboard speed. W has unit of energy if e_p is calibrated with force. Hence, we consider it as work.

We fitted an LMM to each of muscle activation ($C_{11}, \ldots, C_{44}$), co-activation (C_{12}, C_{13}, and C_{24}), the total muscle activation (C_{Total}), and work (W) to investigate motor learning. This model includes condition, leg, and movement direction as fixed intercepts. The interaction between condition and leg is also considered in the model in addition to a fixed slope for the trial number. Similar to the trial elapsed time model (Equation 1), we considered random intercept and slope for capturing the correlation of measurements within each participant. Therefore, the observation i for each of the muscle activation or co-activation (C_{pq}) for the participant m is modeled as

$$C^{im} = \beta_0 + \beta_1 \mathrm{B}_i + \beta_2 \mathrm{A2}_i + \beta_3 \mathrm{left}_i + \beta_4(\mathrm{B}_i, \mathrm{left}_i) + \beta_5(\mathrm{A2}_i, \mathrm{left}_i) + \beta_6 \mathrm{backward}_i + \beta_7 \mathrm{trial}_i + b_{0m}\mathrm{sub}_{im} + b_{1m}(\mathrm{trial}_{im}, \mathrm{sub}_{im}) + \varepsilon_{im}. \quad (2)$$

Further, we investigated the variations of total muscle activation with respect to each leg and condition. To focus on the mean value of the total activation in each condition and leg, we included only intercepts in the model. Fixed intercepts were considered for condition, leg and their interaction. Similar random effects were also considered to account for the correlation of repeated measurements within participants. The resulting model is

$$\begin{aligned} C^{im}_{\mathrm{Total}} = {} & \beta_0 + \beta_1 \mathrm{B}_i + \beta_2 \mathrm{A2}_i + \beta_3 \mathrm{left}_i + \beta_4(\mathrm{B}_i, \mathrm{left}_i) + \beta_5(\mathrm{A2}_i, \mathrm{left}_i) + b_{0m}\mathrm{sub}_{\mathrm{im}} + b_{1m}(\mathrm{B}_{im}, \mathrm{sub}_{\mathrm{im}}) \\ & + b_{2m}(\mathrm{A2}_{im}, \mathrm{sub}_{\mathrm{im}}) + b_{3m}(\mathrm{left}_{im}, \mathrm{sub}_{\mathrm{im}}) + b_{4m}(\mathrm{B}_{im}, \mathrm{left}_{im}, \mathrm{sub}_{\mathrm{im}}) + b_{5m}(\mathrm{A2}_{im}, \mathrm{left}_{im}, \mathrm{sub}_{\mathrm{im}}) + \varepsilon_{im}. \end{aligned} \quad (3)$$

Balance strategy analysis

To investigate how hip and ankle balance strategies were adopted to control the hoverboard, the similarity between each of those joints' motion and hoverboard plates tilt was evaluated. First, a range normalization was applied to all the trajectories within each condition due to different ranges of motion in the ankle, hip, and hoverboard plate or foot orientation. This was done by removing the mean value of each signal and dividing it by its maximum absolute value. Then, different similarity measures were used in the time and frequency domain.

Participant #	7	4	8	10	9	6	1	2	5
A1	9	7	10	7	4	6	4	5	2
B	9	10	8	8	8	6	6	4	3
A2	11	12	9	8	9	6	5	5	4
Total performed trials	29	29	27	23	21	18	15	14	9

Table 1. Number of completed trials at each condition. Participants are sorted based on the total performed trials.

To track the possible phase between the foot orientation and the ankle and the hip angles we used the Hilbert transform[18] to identify the instantaneous phase[19] of the signals. We checked if there was any constant phase difference between the signals, which is a sign of synchronization between them. To compare the phase difference of hip and ankle joints with respect to the foot orientation, we fitted separate LMMs to each of them. We assumed that the phase slope with respect to time indicates the synchrony of the joints with foot orientation. A significant slope indicates an asynchronous motion while a zero (or non-significant) slope indicates synchrony. We included the condition and leg as fixed effect intercepts. Sample time (t_i) is treated as a fixed slope. The measured values (ϕ_{im}) for a given observation i on participant m is modeled as

$$\phi_{im} = \beta_0 + \beta_1 \mathrm{B}_i + \beta_2 \mathrm{A2}_i + \beta_3 \mathrm{left}_i + \beta_4 \mathrm{t}_i + b_{0m}\mathrm{sub}_{im} + b_{1m}(\mathrm{t}_{im}, \mathrm{sub}_{im}) + \varepsilon_{im}. \tag{4}$$

Furthermore, we used the Dynamic Time Warping (DTW) similarity measure[20] which computes the spatial distance between signals regardless of their temporal differences. It is, therefore, robust to possible phase or frequency drifts between signals which has made it a favorite toolbox in speech or gait recognition. Inspired from these applications, we used DTW as a tool for measuring the spatial distance between foot orientation and ankle and hip angles trajectories. To track the changes of distance between the signals, we computed DTW locally within a moving window with length and steps of 33.34s and 0.67s, respectively. We fitted separate LMMs to each of the ankle and hip DTW data in order to compare each joint's similarity to the foot orientation. Hence, the observation i for each computed distance (d) for the participant m is modeled as

$$d_{im} = \beta_0 + \beta_1 \mathrm{B}_i + \beta_2 \mathrm{A2}_i + b_{0m}\mathrm{sub}_{im} + b_{1m}(\mathrm{B}_i, \mathrm{sub}_{im}) + b_{2m}(\mathrm{A2}_i, \mathrm{sub}_{im}) + \varepsilon_{im}. \tag{5}$$

where d_{im} is the local distance between the observation i of hip or ankle joint from the foot orientation.

We adjusted the complexity of the LMMs by performing Log-likelihood Ratio Test and Akaike Information Criterion. The significance of each effect in the model was also tested using F-test at the 5 percent significance level. To identify differences in the comparison of the similarity measures for ankle and hip angles across participants, we used the Wilcoxon Signed Rank test while for comparison of performance measure across subgroups we used the Wilcoxon Rank Sum test. Non-parametric statistical tests were used since Shapiro–Wilk test rejected the normality assumption. All statistical tests were two-sided with a significance level set to $P < 0.05$. Multiple comparisons were accounted for by the Bonferroni adjustment.

Results

Motor performance and motor learning

We computed the performance of each participant by summing the number of completed trials at each condition (Table 1). We also evaluated the motor learning progress of each participant during each condition using the trial elapsed time and the muscle activation (individually and in total). Figures 2A,C illustrate these values for participant #9.

Overall, a decrease in trial elapsed time and muscle activity can be observed as participant #9 performed more trials. In particular, Gastrocnemius medial head muscle activity had a decreasing trend in the left leg during backward motion in condition B. Accordingly, we considered the decrease of the trial elapsed time and total muscle activation as a determinant of motor learning. To investigate the variation trends in these indicators, we fitted LMMs in Equation 1 and Equation 2 to trial elapse time data and total muscle activation data, respectively. There is a significant negative slope both in trial elapsed time and total muscle activation data (F-test:$p_{time} = 8.46e-4$, $p_{TotalEMG} = 8.6e-4$). Figure 4E illustrates the average trial completion time change and the average total muscle activation change for each participant across conditions computed based on the values estimated by corresponding LMMs.

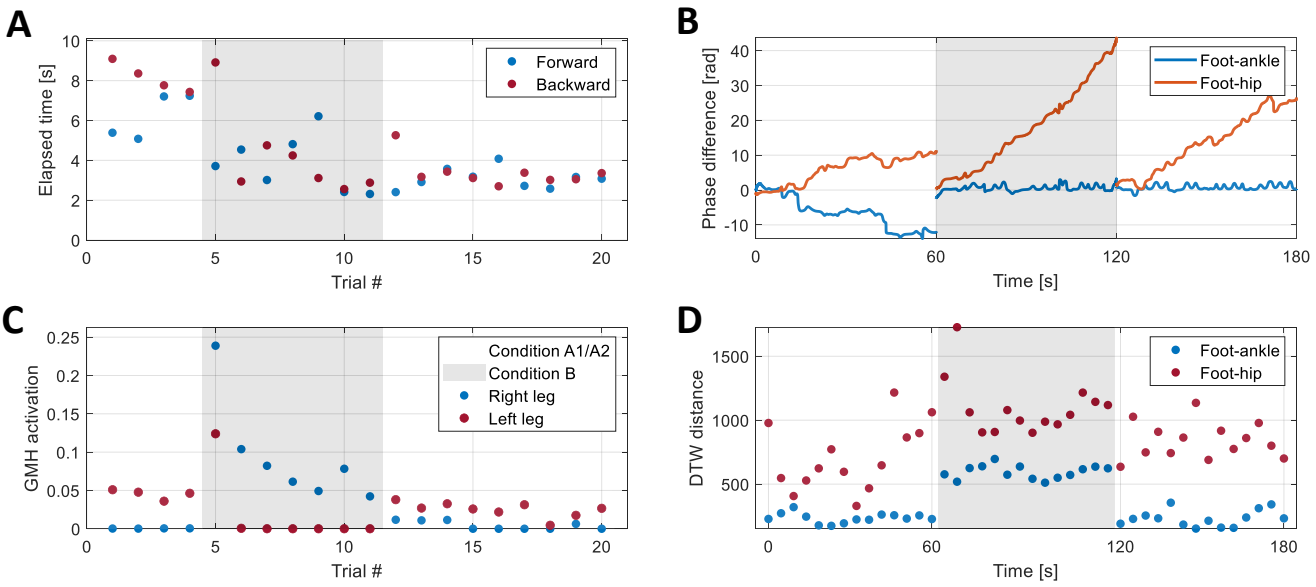

Figure 2. Example data of participant #9: (**A**) Successful trials elapsed time for each forward/backward movement. (**B**) Relative phase difference between the right foot trajectory and ankle and hip angles, respectively. (**C**) Gastrocnemius medial head activation in backward movement in each trial (movements between horizontal Top and Bottom lines). (**D**) DTW distance between the right foot trajectory and ankle and hip angles, respectively.

Adoption of ankle based balance strategy

As described, hoverboard balance is achieved by controlling the tilt angle of its plates. As a result, oscillatory trajectories are expected for hoverboard plates during the forward and backward movements. This oscillatory behavior is not, however, equally mapped into each joint but is reflected mainly based on the adopted balance strategy. In other words, the foot orientation is simultaneously affected by the ankle, knee, and hip angles, so there are infinite ways to control the foot orientation. To investigate the strength of the ankle or hip balance strategy in controlling the hoverboard, we examined how ankle and hip joint trajectories are correlated with foot orientation (i.e. the tilt of the hoverboard plates), by studying their trajectories phase difference and dynamical time warping distance.

Phase difference

We computed the phase difference between the foot orientation and the ankle and hip angles across all participants. Figure 2B shows the phase difference for participant 9. In condition A1, the participant seems to be exploring a proper balance strategy since the phases of both ankle and hip joints were drifting. After learning how to control the hoverboard in condition A1, participant 9 synchronized the ankle movement with the hoverboard plate angle which led to negligible phase difference compared to the hip joint in conditions B and A2. To check if the similar observation is valid over all participants, we fitted the LMM in Equation 4 to each of the ankle and hip joint phase difference data. Figure 4C shows the phase slope for the hip and ankle joints estimated by their corresponding models where the value of each point in the graph is equal to $\beta_4 + b_{1m}$. According to the performed F-test on both models, the slope fix effect does not significantly contribute to the ankle model ($p_{\beta_4,\text{ankle}} = 0.5706$) while the opposite applies to the hip model where there exists a significant positive fix slope ($p_{\beta_4,\text{hip}} = 1.7e-10$). These observations show that a small phase difference from foot orientation is maintained in the ankle while the hip phase is constantly drifting. Therefore, a synchronous motion pattern with the hoverboard plates exists in the ankle joint which is an indicator of the ankle balance strategy.

To further investigate phase data in different conditions and legs, we compared the standard deviation of hip and ankle phases across all participants in Figure 3A. This is also helpful in studying how controlling the hoverboard plates orientation corresponds to an ankle or a hip strategy. As it can be seen in the figure, the hip joint has a higher phase standard deviation than the ankle joint which is significantly representing a more synchronous pattern in comparison to the hip angle in all conditions

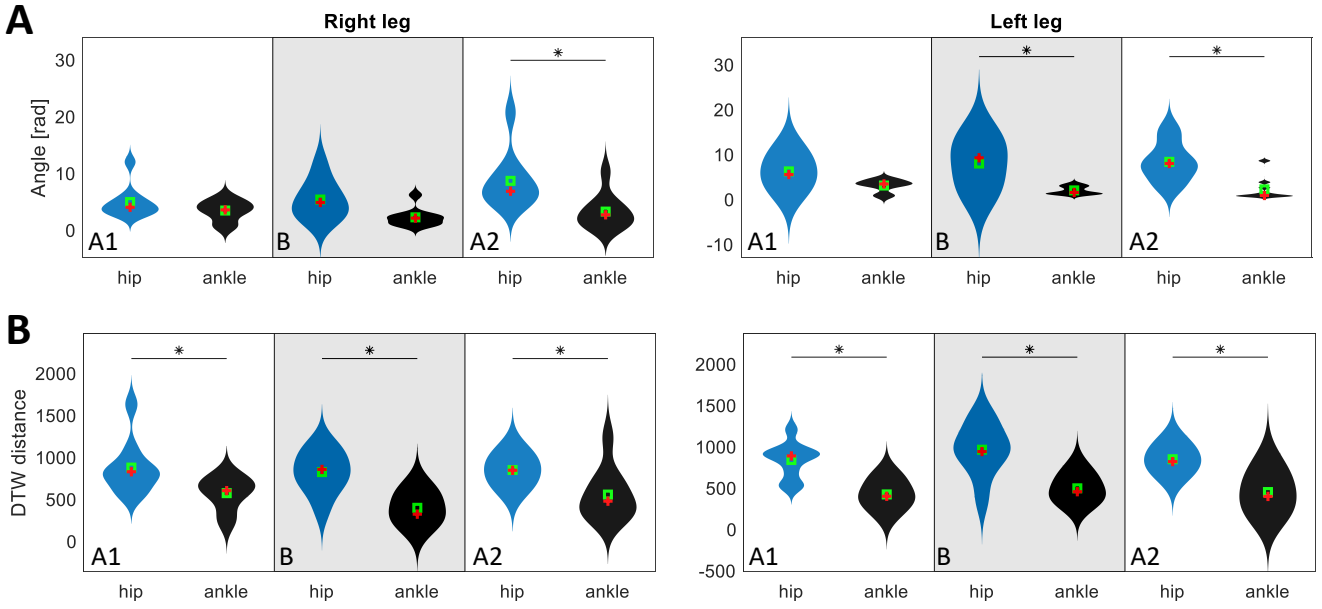

Figure 3. (**A**) Distribution comparison of phase standard deviation between the ankle and hip joints across all participants in the right and left legs. (**B**) Distribution comparison of average DTW distance of the ankle and hip angles from foot orientation across all participants in the right and left legs. Within each violin plot, a cross and a square indicate the median and the mean values, respectively. Asterisks indicate significant difference based on two-tailed Wilcoxon signed rank tests.

both in right (two-tailed Wilcoxon signed rank test, $p_{A1} = 0.6523$, $p_B = 0.0546$, $p_{A2} = 0.0039$) and left leg (two-tailed Wilcoxon signed rank test, $p_{A1} = 0.1289$, $p_B = 0.0273$, $p_{A2} = 0.0390$). This suggests that an ankle balance strategy is used.

DTW distance

DTW is another perspective from which we can examine the balance strategy. We used DTW to measure the distance between the ankle and hip angles and foot orientation. These values are shown for participant 9 in Figure 2D as an example. We notice smaller distances between the ankle and foot trajectories compared to hip angle in all three conditions. Furthermore, the participant is more successful in maintaining larger hip-foot distances compared to the ankle-foot distances as more trials are performed. These observations intuitively confirm learning of the ankle strategy which was previously concluded using phase analysis. We fitted separate LMMs to the DTW data based on Equation 5. Figure 4B shows the overall distance of each of the ankle and hip joint angles from the hoverboard plates orientation. The results show that the hip joint angles have significantly higher distances from the hoverboard plates orientation in comparison to the ankle angles in all conditions (F-test, $p_{A1} = 0.009$, $p_B = 0.003$, $p_{A2} = 0.0001$). This indicates that participants mostly used their ankles in controlling the hoverboard plates which consequently implies that an ankle balance strategy is adopted.

To further analyze the above results, we compared the mean distances of hip and the ankle joint angles from hoverboard plates orientation in each condition and leg separately. According to Figure 3B, ankle angle trajectory has significantly a lower distance from the foot orientation in comparison to the hip angle distance for both the right (two-tailed Wilcoxon signed rank test, $p_{A1} = 0.0273$, $p_B = 0.0078$, $p_{A2} = 0.0117$) and the left (two-tailed Wilcoxon signed rank test, $p_{A1} = 0.0078$, $p_B = 0.0078$, $p_{A2} = 0.0117$) legs in all conditions.

Muscle activation

This subsection investigates how the adoption of the ankle balance strategy was reflected in muscle activation data. We fitted an LMM to the activation and co-activation data according to Equation 2. Figure 4A shows the slope of muscle activation evolution over performed trials for each of the muscle activation and co-activation ($\beta_7 + b_{1m}$). The majority of estimated slopes

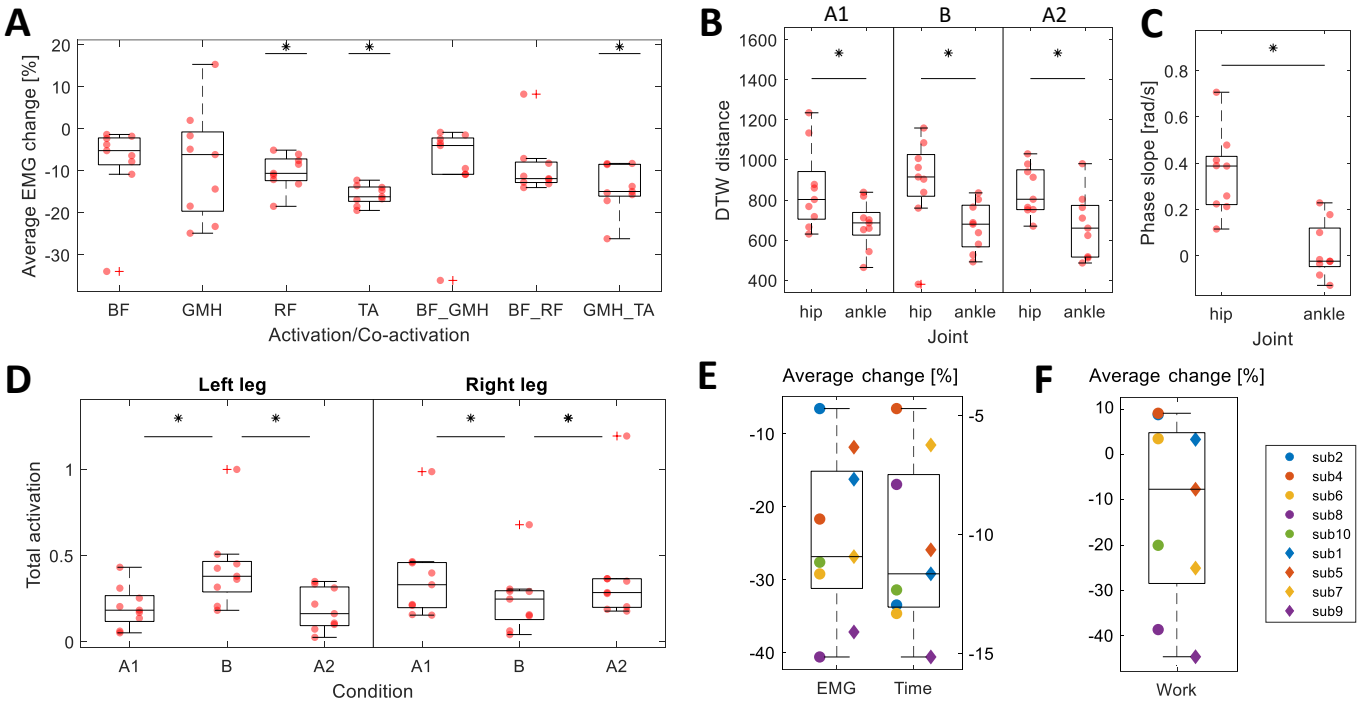

Figure 4. (**A**) Muscle activation slope effect (rate of activation change over trials) for each activation/co-activation across participants. (**B**) Comparison of average estimated values of the DTW distance for the hip and ankle joints across participants. (**C**) Comparison of estimated phase slopes for the hip and ankle joints (the rate of phase change over sample time) across participants. (**D**) Average total muscle activation in each condition and leg across participants. (**E**) Comparison of the average decrease in trial elapse time and the total muscle activation over trials across participants. (**F**) Average decrease in work over trials across participants.

are negative. Although the slope is not significant for all the muscle activation/co-activation, it exhibits a decreasing trend in muscle effort which is an indicator of learning. In particular, the ankle joint co-activation has a significant decreasing slope (F-test, p_{GMH_TA}=0.0092). This signifies the learning of movement in the ankle joint which is consequently an outcome of adopting the ankle balance strategy.

In the fitted model, all of the fixed effects are significantly contributing to the model but those related to condition A2 meaning that it is not significantly different from A1 and its related intercepts provide the model with no extra degree of freedom. This suggests that participants successfully retrieved the strategy learned in A1 when they performed trials in the A2 condition. To further analyze this, we computed the total muscle activation and fitted the LMM in Equation 3 to total activation data. Figure 4D shows the mean value for each participant's total activation in different conditions and legs. According to the figure, the estimated total activation in condition B is significantly different from conditions A1 and A2 for both legs ($p_{A1R,BR}$=0.0088, $p_{A2R,BR}$=0.0294, $p_{A1L,BL}$=0.0074, $p_{A2L,BL}$=0.0047) while conditions A1 and A2 do not have a significant difference in activation/co-activation ($p_{A1R,A2R}$=0.3665, $p_{A1L,A2L}$=0.7050).

Discussion

motor learning

We observe in Figure 4E that the time for one trial decreased across participants of $-10.56 \pm 4.10\%$, which yields a significant improvement of performance. However, does this improvement come at the cost of increased effort? As the work is not increased for majority of participants (Figure 4F, work decreased of 10% to 45% in 6 participants, versus increase of only 5% to 10% in 3 participants) and muscle activation decreased across all subjects of $-24.23 \pm 11.26\%$, this indicates learning with skill improvement. We further investigated motor learning by analyzing the co-activation, which is arguably high at the initial

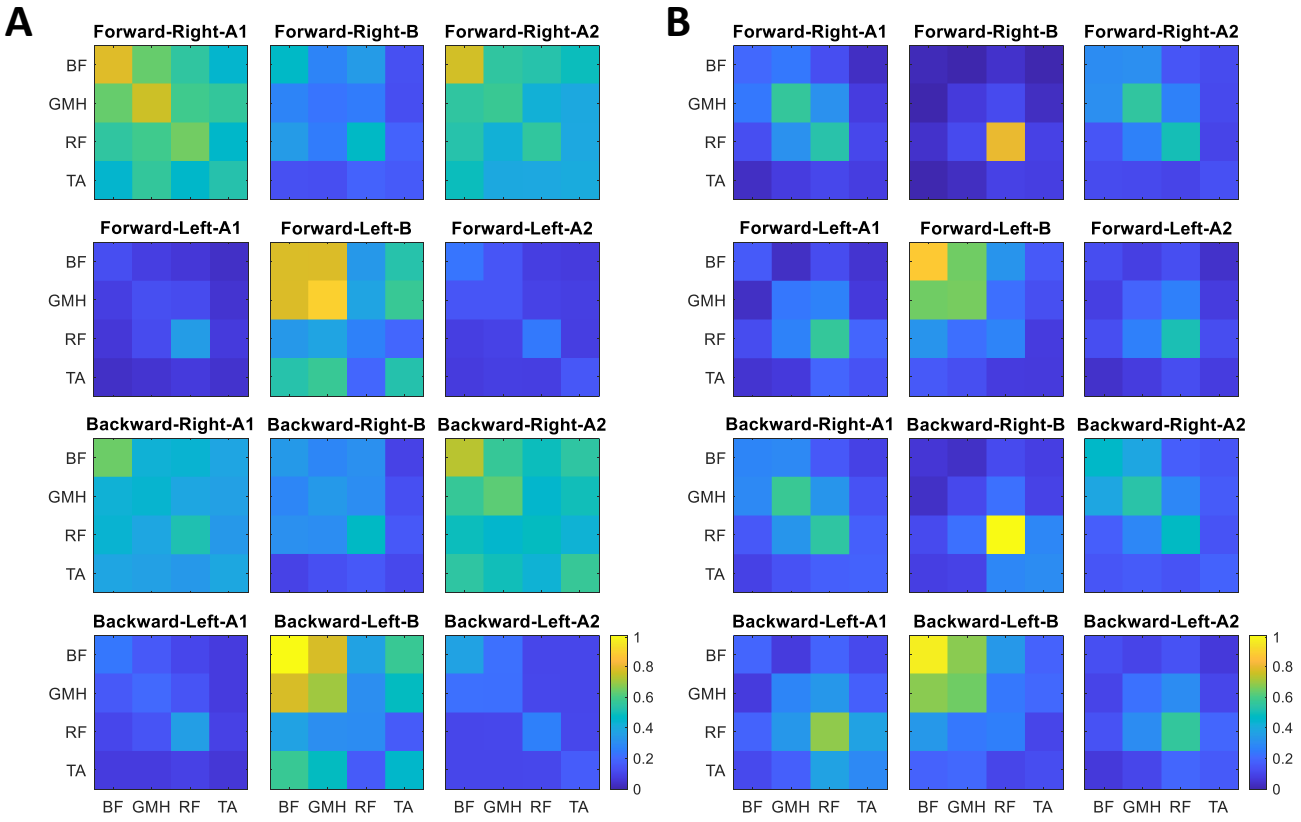

Figure 5. Average muscle activation (co-activation) patterns separated based on movement direction, leg, and condition for (**A**) LP group and (**B**) HP group.

stages of dealing with unknown unstable tasks[21]. Generally, this enables the motor system to maintain the movement close to the planed trajectory until the feedforward control of muscle activation is shaped[22]. In this context, we note that the decrease of co-activation in the ankle joint of $-14.20 \pm 5.68\%$ (Figure 4A) revealing effort minimization in this most important joint for the hoverboard control task.

Robustness of adopted balance strategy

A-B-A paradigm was used in this study to investigate if the adoption of a balance strategy depends on the participants' initial posture, and to check whether they can retain their motor memory obtained in the A1 condition and use it in the similar condition of A2 (while they had been exposed to a different posture and muscle activation patterns in between). According to Figure 4D, the muscle activation in condition B is different from the A1 and A2 conditions. Different muscle activation in condition B and the significant difficulty of participants in performing the early trials in this condition, manifested by increased elapsed time and far from straight line hoverboard trajectories, suggests that condition B can be considered as a novel task. This indicates that the adopted strategy is robust to different muscle activation patterns and kinematics as ankle based balance strategy is adopted regardless of the condition factor.

Furthermore, no motor memory interference occurred. Switching from condition A1 to condition B, participants face a novel task that requires a new motor learning that leads to different patterns of muscle activation. Switching from condition B to condition A2, we observe muscle activation patterns are the same as the A1 condition. This indicated that the captured motor memory in the A1 condition does not interfere with the one from condition B, and participants were able to retrieve the captured motor memory in A1 and use it in A2.

High and low performance groups

Furthermore, we studied the correlation between the strength of the adopted ankle balance strategy and the performance of participants. In this regard, a K-means clustering was applied to the number of successful trials across conditions which divided the participants into two groups of high performance (HP) and low performance (LP) (Group HP: participants number 4,7,8,9, and 10). Based on a comparison of features such as standard deviation of instantaneous phase and the average distance between the ankle and hip angle trajectories, we observed that the HP group has more clearly adopted an ankle balance strategy in comparison to the LP group. Furthermore, we observed that the HP group had lower muscle co-activation in their ankle which implies lower stiffness at the ankle joint indicating motor learning[21]. Interestingly, work can also discriminate HP and LP participants. According to Figure 4F, LP participants had negligible decrease in work while HP participants' work dropped between 20% to 45% (Participant #4 was an exception who did not exhibit a considerable reduction in work).These observations corroborate our conclusion that by adopting a more clear ankle based balance strategy, HP improved performance in comparison to the LP participants.

The participants' average muscle recruitment patterns can be further analyzed. Figure 5A and Figure 5B show the average normalized muscle activation patterns of LP and HP groups, respectively. As we see in these figures, the right leg's muscles are more active in A1 and A2 conditions while the left leg's muscles are more active in condition B. Therefore, we can consider the right leg as the dominant leg in balance control in A1 and A2 conditions while the left leg is the dominant leg in balance control in condition B. Furthermore, we observed that HP participants tend to activate a lower number of muscles simultaneously while LP group recruit more muscles. This could be a determinant of lower co-activation in HP participants in comparison to the LP participants and a sign of more motor exploration in the LP group.

kinematic measures and performance metrics

We evaluated participants' performance based on various kinematic metrics such as maximum perpendicular deviation, maximum line crossing error, average hoverboard orientation, and line crossing angles but none of them were able to discriminate participants in a meaningful way. The underlying reason is that riding a hoverboard is more complicated than a simple point-to-point reaching movement. In this novel task, participants have a large number of degrees of freedom in performing a trial which is moving between two lines without any constraint (see Figure 1E as an example of movement in the x-y plane). This leads to a variety of strategies and patterns observable in their movement path. This suggests that learning could happen as a change in the method of redundancy resolution through the adoption of an appropriate strategy rather than a decrement in kinematic error. Furthermore, due to the complexity of the task, it probably takes more time than usual point-to-point movements that motor learning signs emerge in kinematic data. However, the analysis of time and total muscle activation data gave important information on motor learning and performance.

Conclusion

This work investigates the learning of lower limb motor control and dynamic balance in first-time hoverboard riders. 10 participants were asked to perform goal-oriented back and forth movements in 60 seconds using a hoverboard. Decreased total muscle activation, trial elapsed time, and ankle joint co-activation over the performed trials indicated the occurrence of motor learning which according to phase synchrony and DTW analysis, emerged itself as adoption of ankle balance strategy. The learned ankle strategy was robust to performing the task with a different foot orientation. Further analysis suggested that the strength of the ankle strategy correlates with the performance of the participants. Results of this paper provides us deeper understanding with regard to the neuromechanics of hoverboard riding.

References

1. van der Kooij, H., Jacobs, R., Koopman, B. & Grootenboer, H. A multisensory integration model of human stance control. *Biol. Cybern.* **80**, 299–308 (1999).
2. Peterka, R. Sensorimotor integration in human postural control. *J. Neurophysiol.* **88**, 1097–1118 (2002).
3. Kuo, A. D. An optimal state estimation model of sensory integration in human postural balance. *J. Neural Eng.* **2**, S235 (2005).

4. Winter, D. A. Human balance and posture control during standing and walking. *Gait Posture* **3**, 193–214 (1995).
5. Sullivan, B., Harding, A. G., Dingley, J. & Gras, L. Z. Improvements in dynamic balance using an adaptive snowboard with the nintendo wii. *Games for Heal. Res. Dev. Clin. Appl.* **1**, 269–273 (2012).
6. Kinzey, S. J. & Armstrong, C. W. The reliability of the star-excursion test in assessing dynamic balance. *J. Orthop. Sports Phys. Ther.* **27**, 356–360 (1998).
7. Davlin, C. D. Dynamic balance in high level athletes. *Percept. Mot. Ski.* **98**, 1171–1176 (2004).
8. Rahman, K. A., Azaman, A., Mohd Latip, H., Mat Dzahir, M. & Balakrishnan, M. Comparison of tibialis anterior and gastrocnemius muscles activation on balance training devices and hoverboard. *Malays. J. Fundam. Appl. Sci* **13**, 495–500 (2017).
9. Horak, F. B. & Nashner, L. M. Central programming of postural movements: adaptation to altered support-surface configurations. *J. Neurophysiol.* **55**, 1369–1381 (1986).
10. Burdet, E., Osu, R., Franklin, D. W., Milner, T. E. & Kawato, M. The central nervous system stabilizes unstable dynamics by learning optimal impedance. *Nature* **414**, 446–449 (2001).
11. Lee, H., Ho, P., Rastgaar, M., Krebs, H. I. & Hogan, N. Multivariable static ankle mechanical impedance with active muscles. *IEEE Transactions on Neural Syst. Rehabil. Eng.* **22**, 44–52 (2013).
12. Amiri, P. & Kearney, R. E. Ankle intrinsic stiffness changes with postural sway. *J. Biomech.* **85**, 50–58 (2019).
13. Huang, H. Y., Arami, A., Farkhatdinov, I., Formica, D. & Burdet, E. The influence of posture, applied force and perturbation direction on hip joint viscoelasticity. *IEEE Transactions on Neural Syst. Rehabil. Eng.* **28**, 1138–1145 (2020).
14. Lee, H., Rouse, E. J. & Krebs, H. I. Summary of human ankle mechanical impedance during walking. *IEEE J. Transl. Eng. Heal. Medicine* **4**, 1–7 (2016).
15. Arami, A., van Asseldonk, E., van der Kooij, H. & Burdet, E. A clustering-based approach to identify joint impedance during walking. *IEEE Transactions on Neural Syst. Rehabil. Eng.* **28**, 1808–1816 (2020).
16. Chagdes, J. R., Rietdyk, S., Jeffrey, M. H., Howard, N. Z. & Raman, A. Dynamic stability of a human standing on a balance board. *J. Biomech.* **46**, 2593–2602 (2013).
17. Konrad, P. The abc of EMG: A practical introduction to kinesiological electromyography (2005). Available at https://www.noraxon.com/wp-content/uploads/2014/12/ABC-EMG-ISBN.pdf.
18. Oppenheim, A. V. *Discrete-time signal processing* (Pearson Education India, 1999).
19. Marple, L. Computing the discrete-time" analytic" signal via fft. *IEEE Transactions on Signal Process.* **47**, 2600–2603 (1999).
20. Sakoe, H. & Chiba, S. Dynamic programming algorithm optimization for spoken word recognition. *IEEE Transactions on Acoust. Speech, Signal Process.* **26**, 43–49 (1978).
21. Heald, J. B., Franklin, D. W. & Wolpert, D. M. Increasing muscle co-contraction speeds up internal model acquisition during dynamic motor learning. *Sci. Reports* **8**, 1–11 (2018).
22. Franklin, D. W. *et al.* Cns learns stable, accurate, and efficient movements using a simple algorithm. *J. Neurosci.* **28**, 11165–11173 (2008).

Acknowledgements

Author contributions

A.A. and A.T. designed the experiments, J.L. and A.A. conducted the experiments, M.S. analyzed the results. All authors were involved in interpreting the results and the preparation of the manuscript.

Competing interests

The authors declare no competing interests.

Additional information

Correspondence and requests for materials should be addressed to M.S and A.A.